BEHAVIOUR OF VARIOUS CATHODE MATERIALS FOR NON-AQUEOUS LITHIUM CELLS

HIRONOSUKE IKEDA and SATOSHI NARUKAWA

Sanyo Electric Co., Ltd., Shioya Research Center 809-332, Aza-takamaru, Higashitarumi-cho, Tarumiku, Kobe-shi, Hyogo (Japan)

(Received June 23, 1982; in revised form November 6, 1982)

Summary

The reaction mechanisms with Li of various metal oxides, sulfides and a selenide in nonaqueous electrolyte have been studied by the galvanostatic method, X-ray diffraction analysis, and ion-microanalysis. As a result, cell reactions were classified into 3 types. (1) The directly reduced type: cathode materials are reduced directly to metal; CuO, etc. (2) The 2 step reaction type: reaction proceeds through intermediate products: FeS_2 (3) The solid diffusion type, based on the so-called intercalation reaction; MnO_2, TiS_2, etc.

Introduction

Various kinds of halogenides, sulfides, and oxides which assume the solid, liquid and gaseous state have been studied as cathode active materials for lithium cells for approximately 10 years. In the past 5 years, the development of these cells had advanced rapidly and they have become increasingly popular world-wide for consumer use.

At present, lithium cells in practical use are 3 V systems.

Recently, some 1.5 V system lithium cells have been put into practical use. At the same time the reaction mechanisms of various lithium cell systems have been gradually clarified.

The authors have developed the MnO_2/Li cell and popularized it world-wide. For cathode material, we selected solid active MnO_2 from the point of view of stability. We have already presented the reaction mechanism of the MnO_2/Li cell in detail [1 - 3]. We have also studied other solid active materials and have presented the results in part [4].

Following subsequent investigations, we have obtained some different reaction mechanisms. The detailed reaction mechanisms are presented below.

Experimental

Cathode active materials

Oxides: MnO_2, MoO_3, WO_3, TiO_2, CuO, Bi_2O_3, V_6O_{13}; sulfides: FeS_2, TiS_2; selenide: $NbSe$. These electrodes were dried under vacuum at 250 - 300 °C.

Electrolyte

As electrolyte, $LiClO_4$ or another lithium compound was dissolved in a mixed solvent of propylene carbonate (PC) and another organic solvent.

The electrolyte used contained less than 50 ppm H_2O. The following characteristics of the materials were measured as half cells or lithium cells, to evaluate cell characteristics and to determine reaction mechanisms: galvanostatic method, discharge characteristics; X-ray diffraction analysis, cell performance; ion-microanalysis.

Results and discussion

(i) X-ray diffraction analysis

Figures 1 - 3 show X-ray diffraction patterns at various stages of discharge of several cathode mixes of test cells. Here, MnO_2, FeS_2 and CuO are conceivably the most typical from the viewpoint of discharge performance, reaction mechanism, etc.

As the discharge proceeds, the peaks seen at 0% utilization shift to lower angles (Fig. 1): that is, an expansion of the crystal lattice is observed. These results have already been reported [1].
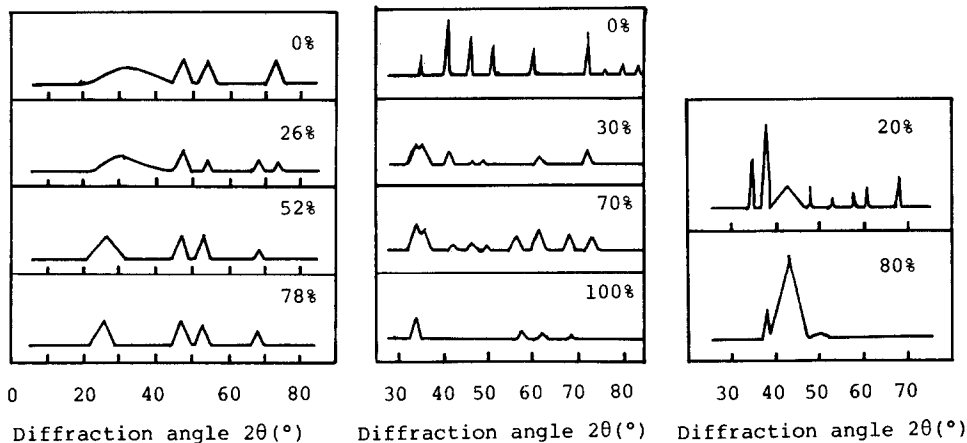

Fig. 1. X-ray diffraction patterns for $\gamma \cdot \beta$-MnO_2 at various discharge depths.

Fig. 2. X-ray diffraction patterns of FeS_2 at various discharge depths.

Fig. 3. X-ray diffraction patterns of CuO at various discharge depths.

In Fig. 2 for FeS_2, it can be seen that at 30% discharge depth, the Li_2S peaks are not yet apparent. At 70% depth of discharge, the Li_2S peaks have appeared.

These results suggest the presence of intermediate products.

From Fig. 3 for CuO, at 20% depth of discharge, the peak due to Cu metal has already appeared, and at the 80% discharge stage, the peak becomes extremely strong. This suggests that the CuO has been reduced to metallic Cu by direct reaction.

(ii) Ion microanalysis

Figures 4 - 6 show the micro-transition of cathode mixtures of MnO_2, FeS_2 and CuO at various stages of the discharge reaction.

Figure 4 compares Li^+ and Mn^+ ion images obtained by IMA. Interrelations between the Li^+ and Mn^+ ion images are observed. It is clear from the results of X-ray diffraction analysis, which shows the shifting of peaks and no Li_2O and Mn_2O_3, and IMA analysis, that the discharge mechanism of MnO_2/Li cells is as follows:

$$Li + Mn^{IV}O_2 \longrightarrow Mn^{III}O_2(Li^+)$$
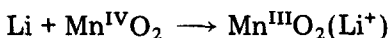
which the authors have proposed previously [1]. $Mn^{III}O_2(Li^+)$ signifies that the Li^+ ion was introduced into the MnO_2 crystal lattice, and Mn was reduced to the trivalent state from the tetravalent state by the Li^+ ion.

Figure 5 shows the interrelations between the Fe^+ and Li^+ ion images observed at 20% discharge depth. These interrelations became weaker as the discharge proceeded.

This supports the following reaction mechanism. The Li^+ ion is introduced into the FeS_2 crystal lattice to form an intermediate product similar to a solid solution. After further reaction, Fe and Li_2S are gradually deposited.

From the above results, the reaction mechanisms for the FeS_2/Li cell are as follows: the reaction produces intermediate products.

$$4Li + FeS_2 \longrightarrow 2Li + \underset{\underset{\displaystyle S-Li}{|}}{\overset{\overset{\displaystyle S-Li}{|}}{Fe}} \longrightarrow Fe + 2Li_2S.$$
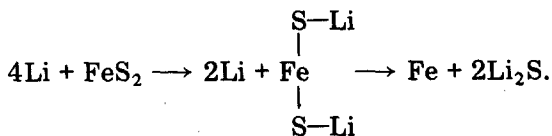
For the CuO/Li cell, the normal reaction mechanism applies (Fig. 6).

$$2Li + CuO \longrightarrow Cu + Li_2O.$$
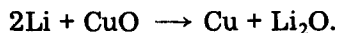
(iii) Charge–discharge characteristics

To study the fundamental performances of the various earlier described cathode materials, various electrodes were measured by the galvanostatic charge–discharge test. Figure 7 shows charge and discharge curves for MoO_3. The reversibility is readily apparent.
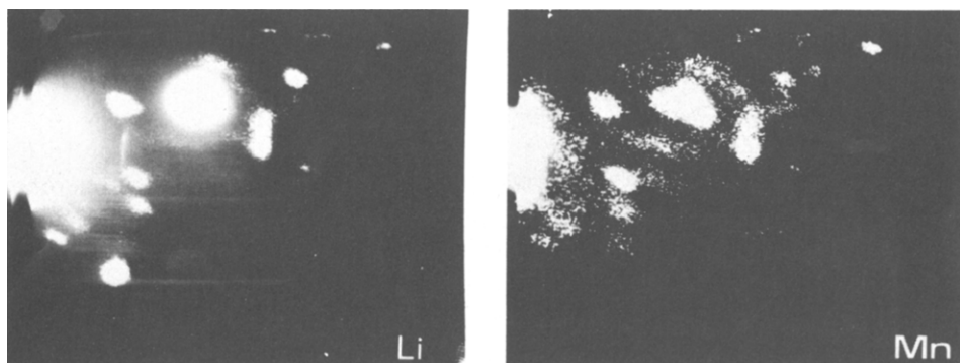
Fig. 4. Specific ion images in MnO_2 mixtures at 80% discharge depth.
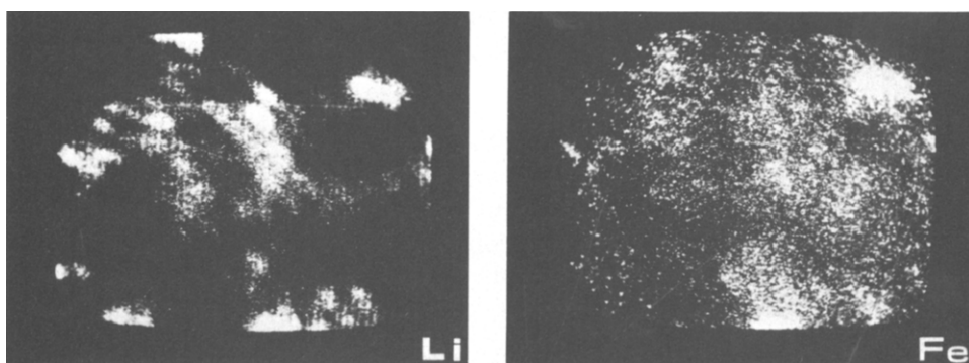

Fig. 5. Specific ion images in FeS_2 at 20% discharge depth.
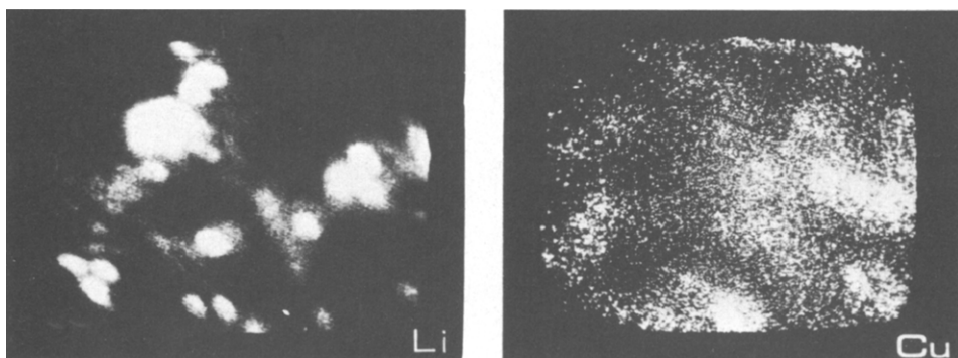

Fig. 6. Specific ion images in CuO mixture at 20% discharge depth.

In another measurement, the Li^+ ion was introduced into various cathode test materials, and the Li concentration ratio in the reaction products was measured by IMA. Figure 8 shows this for MoO_3, and the intensity ratio of Li is correlated to the X value.
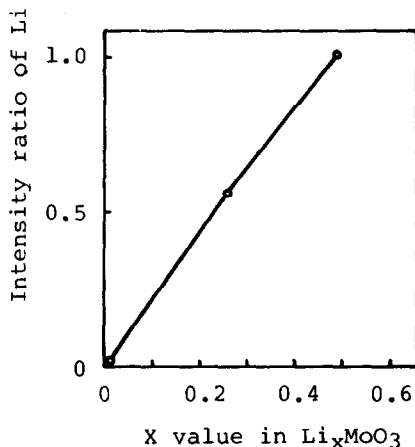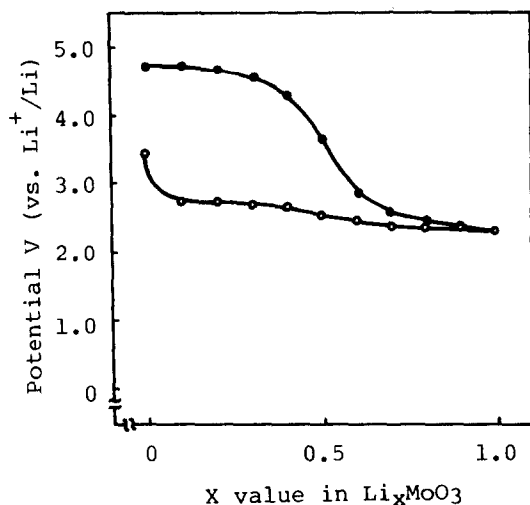
Fig. 7. Charge and discharge curve for MoO_3. ●, Charge; ○, discharge.

Fig. 8. Lithium concentration from IMA analysis of cathode.

Using the above measurements, we have studied the cycling behaviour, particularly of the materials that undergo an intercalation reaction.

We studied MnO_2, WO_3, TiO_2, V_6O_{13}, TiS_2 and NbSe, and confirmed that these materials undergo an intercalation reaction as reported previously [5 - 9].

Conclusion

From the results of the measurements described above, the following summarized conclusions have been drawn.

(a) The introduction of the Li^+ ion into the crystal lattice according to the proposed reaction has been confirmed for MnO_2, WO_3, TiO_2, MoO_3, V_6O_{13}, TiS_2 and NbSe.

(b) From measurements during the cycling test, the entry and exit of the Li^+ ion into and from the crystal lattice were almost quantitatively equal, so the above materials were considered to produce similar products to MnO_2-(Li) as described by the author [1].

(c) In addition, as previously described for CuO, CuO and Bi_2O_3 were reduced directly by Li to produce the metal and Li_2O. These reaction equations are, in general, as follows.

$$Li + MX \longrightarrow M + LiX \qquad M = Metal, X = O_x, S_x, etc.$$
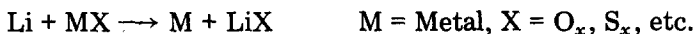
(d) The formation of intermediate products was observed in the discharge of FeS_2, and in the final stage the metal and sulfide were produced. This reaction equation is shown, in general, as:

$$Li + MX \longrightarrow Li + MXLi \longrightarrow M + LiX.$$

(e) From the above, as a general classification, 3 reaction types have been observed. The differences between these reaction systems are considered to be very important in the design of cells.

(f) Cathode materials for lithium cells that have an intercalation reaction mechanism were considered to have the following general equation.

$$MXLi \underset{discharge}{\overset{charge}{\rightleftharpoons}} MX + Li$$
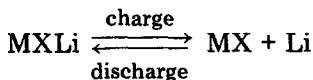
The materials which obey this equation are suitable for use in secondary lithium cells.

References

1 H. Ikeda, T. Saito and H. Tamura, *Manganese Dioxide Symposium, Cleveland, 1975*, Vol. 1, I.C. Sample Office c/o Union Carbide Corporation, Cleveland, Ohio, 1975, p. 384.
2 H. Ikeda, M. Hara and S. Narukawa, *Proc. 28th Power Sources Symp., Atlantic City, NJ, 1978*, The Electrochemical Society Inc., Princeton, NJ, 1978, p. 210.
3 H. Ikeda and S. Narukawa, *Workshop on Lithium Nonaqueous Battery Electrochemistry, Cleveland, 1980*, The Electrochemical Society Inc., Princeton, NJ, 1980, p. 110.
4 H. Ikeda, M. Hara, S. Narukawa, S. Nakaido and N. Hurukawa, *19th Battery Symposium, Tokyo, 1978*, The Japanese Battery Committee, Tokyo, 1978, p. 58.
5 D. M. Murphy, *Workshop on Lithium Nonaqueous Battery Electrochemistry, Cleveland, 1980*, The Electrochemical Society Inc., Princeton, NJ, 1980, p. 197.
6 M. S. Whittingham, *Workshop on Lithium Nonaqueous Battery Electrochemistry, Cleveland, 1980*, The Electrochemical Society Inc., Princeton, NJ, 1980, p. 206.
7 S. Yamanaka, *21st Battery Symposium, Okayama, 1980*, The Japanese Battery Committee, 1980, p. 81.
8 K. Sasaki and H. Nishihara, *22nd Battery Symposium, Kyoto, 1981*, The Japanese Battery Committee, 1981, p. 143.
9 H. Ikeda, H. Tamura, S. Narukawa, T. Hara and H. Yoneyama, *22nd Battery Symposium, Kyoto, 1981*, The Japanese Battery Committee, 1981, p. 105.